Quasiparticle Lifetime of the Repulsive Fermi Polaron

Haydn S. Adlong,[1] Weizhe Edward Liu,[1,2] Francesco Scazza,[3] Matteo Zaccanti,[3] Nelson Darkwah Oppong,[4,5,6] Simon Fölling,[4,5,6] Meera M. Parish,[1,2] and Jesper Levinsen[1,2]

[1]*School of Physics and Astronomy, Monash University, Victoria 3800, Australia*
[2]*ARC Centre of Excellence in Future Low-Energy Electronics Technologies, Monash University, Victoria 3800, Australia*
[3]*Istituto Nazionale di Ottica del Consiglio Nazionale delle Ricerche (CNR-INO) and European Laboratory for Nonlinear Spectroscopy (LENS), 50019 Sesto Fiorentino, Italy*
[4]*Ludwig-Maximilians-Universität, Schellingstraße 4, 80799 München, Germany*
[5]*Max-Planck-Institut für Quantenoptik, Hans-Kopfermann-Straße 1, 85748 Garching, Germany*
[6]*Munich Center for Quantum Science and Technology (MCQST), Schellingstraße 4, 80799 München, Germany*

(Received 1 May 2020; revised 20 July 2020; accepted 24 August 2020; published 24 September 2020)

We investigate the metastable repulsive branch of a mobile impurity coupled to a degenerate Fermi gas via short-range interactions. We show that the quasiparticle lifetime of this repulsive Fermi polaron can be experimentally probed by driving Rabi oscillations between weakly and strongly interacting impurity states. Using a time-dependent variational approach, we find that we can accurately model the impurity Rabi oscillations that were recently measured for repulsive Fermi polarons in both two and three dimensions. Crucially, our theoretical description does not include relaxation processes to the lower-lying attractive branch. Thus, the theory-experiment agreement demonstrates that the quasiparticle lifetime is dominated by many-body dephasing within the upper repulsive branch rather than by relaxation from the upper branch itself. Our findings shed light on recent experimental observations of persistent repulsive correlations, and have important consequences for the nature and stability of the strongly repulsive Fermi gas.

DOI: 10.1103/PhysRevLett.125.133401

The concept of the quasiparticle is a powerful tool for describing interacting many-body quantum systems. Most notably, it forms the basis of Fermi liquid theory [1], a highly successful phenomenological description of interacting Fermi systems ranging from liquid ^{3}He to electrons in semiconductors. Here, the underlying particles are "dressed" by many-body excitations to form weakly interacting quasiparticles with modified properties such as a finite lifetime and an effective mass. However, during the past few decades, many materials have emerged that defy a conventional explanation within Fermi liquid theory [2,3]. Therefore, it is important to understand how quasiparticles can lose their coherence or break down.

Quantum impurities in quantum gases provide an ideal testbed in which to investigate quasiparticles since the impurity-medium interactions can be tuned to controllably create dressed impurity particles or *polarons* [4]. To date, there have been a multitude of successful cold-atom experiments on impurities coupled to Fermi [5–17] and Bose [18–22] gases, which are termed Fermi and Bose polarons, respectively. In particular, Fermi-polaron experiments have observed the real-time formation of quasiparticles [13] and the disappearance of quasiparticles in the spectral response with increasing temperature [15]. The Fermi-polaron scenario has even been extended beyond cold atoms, having recently been realized in charge-tunable atomically thin semiconductors [23]. While the ground state of the Fermi polaron (corresponding to the attractive branch) is generally well understood [24–32], there has been much debate about the nature of the metastable repulsive branch [30,33–38], with experiments suggesting that it can be remarkably long lived for a range of interactions [7,14,16]. The stability of this branch is important for realizing Fermi gases with strong repulsive interactions [4,39–43].

In this Letter, we show that the lifetime of the repulsive branch itself is typically much longer than the *quasiparticle lifetime*, which corresponds to the timescale over which the repulsive polaron remains a coherent quasiparticle. The character of the quasiparticle can be probed by driving Rabi oscillations between different internal states of the impurity atom (see Fig. 1), where only one of the states strongly interacts with the surrounding Fermi gas. Previous works have found that the Rabi frequency Ω provides a sensitive probe of the quasiparticle residue Z (squared overlap with the noninteracting impurity state) [7]. Here we demonstrate that the damping rate of oscillations Γ_R is directly linked to the width of the polaron peak in the spectral function, as depicted in Fig. 1(b), which corresponds to the inverse quasiparticle lifetime Γ.

Using a recently developed variational approach [44], we model the Rabi oscillations for two different Fermi-polaron experimental setups: a three-dimensional (3D) ^{6}Li gas with a broad Feshbach resonance [14], and a

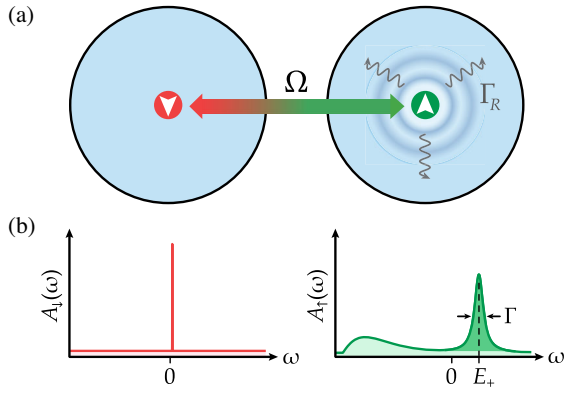

FIG. 1. (a) Two pseudospin states (red and green) of an impurity embedded in a medium (blue) are coupled together and undergo Rabi oscillations with an effective frequency Ω and damping rate Γ_R. (b) The impurity spectral function of a nearly free impurity (left) is coupled to that of an impurity that strongly interacts with the Fermi gas (right). The repulsive polaron peak is centered at energy E_+ above the molecule-hole continuum and is characterized by the residue Z (dark green area) and width Γ [35].

quasi-two-dimensional (2D) ^{173}Yb gas [16] with an orbital Feshbach resonance [45]. We find that we can capture the Rabi dynamics observed in both experiments, correctly reproducing both Ω and Γ_R even though our approximation neglects relaxation processes to the lower attractive branch at negative energies. We furthermore show that the repulsive polaron in the weak-coupling limit is essentially equivalent to the scenario of a discrete state coupled to a continuum, which differs from the usual Fermi-liquid scenario. Thus, we conclude that the quasiparticle lifetime of the repulsive Fermi polaron in two and three dimensions is primarily limited by many-body dephasing within the upper repulsive branch while relaxation to the attractive branch is negligible, in contrast to the prevailing wisdom (see, e.g., Ref. [4] for a review).

Model.—To model the impurity dynamics in the 3D ^{6}Li experiment of Ref. [14] and the 2D ^{173}Yb experiment of Ref. [16], we use a unified notation where the dimensionality of momenta and sums are implicit. For clarity, even though we consider homonuclear systems, we introduce majority fermion creation operators $\hat{f}^\dagger_{\mathbf{k}}$ and impurity creation operators $\hat{c}^\dagger_{\mathbf{k},\sigma}$ with two different pseudospins $\sigma = \uparrow, \downarrow$ (Fig. 1). For a description of the precise relationship to atomic states in experiments, see the Supplemental Material [46].

The Hamiltonian we consider consists of four terms:

$$\hat{H} = \hat{H}_0 + \hat{H}_\uparrow + \hat{H}_\downarrow + \hat{H}_\Omega. \tag{1}$$

The term $\hat{H}_0 = \sum_{\mathbf{k}} (\epsilon_{\mathbf{k}} - \mu) \hat{f}^\dagger_{\mathbf{k}} \hat{f}_{\mathbf{k}}$ describes the medium in the absence of the impurity. Here, $\mathbf{k}$ is the particle momentum, $\epsilon_{\mathbf{k}} = |\mathbf{k}|^2/2m \equiv k^2/2m$ is the kinetic energy, and m is the mass of both the fermions and the impurity (we work in units where $\hbar$ and the system volume or area are set to 1). We use a grand canonical formulation for the medium, with μ the corresponding chemical potential [52,53].

The impurity spin-σ terms

$$\hat{H}_\sigma = \sum_{\mathbf{k}} [\epsilon_{\mathbf{k}} \hat{c}^\dagger_{\mathbf{k}\sigma} \hat{c}_{\mathbf{k}\sigma} + (\epsilon_{\mathbf{k}}/2 + \nu_\sigma) \hat{d}^\dagger_{\mathbf{k}\sigma} \hat{d}_{\mathbf{k}\sigma}] + g_\sigma \sum_{\mathbf{k},\mathbf{q}} (\hat{d}^\dagger_{\mathbf{q}\sigma} \hat{c}_{\mathbf{q}-\mathbf{k}\sigma} \hat{f}_{\mathbf{k}} + \hat{f}^\dagger_{\mathbf{k}} \hat{c}^\dagger_{\mathbf{q}-\mathbf{k}\sigma} \hat{d}_{\mathbf{q}\sigma}), \tag{2}$$

describe the interaction of the impurity and majority fermions via the coupling into a closed channel with creation operator $\hat{d}^\dagger_{\mathbf{k}\sigma}$, where we have coupling constant g_σ and closed-channel detuning ν_σ. Renormalizing the model enables us to trade the bare parameters of the model—the detuning, the coupling constant, and an ultraviolet momentum cutoff—for the physical interaction parameters which parametrize the 2D and 3D impurity-majority fermion low-energy scattering amplitudes

$$f_{2\mathrm{D}\sigma}(k) \simeq \frac{4\pi}{-\ln(k^2 a^2_{2\mathrm{D}\sigma}) + R^2_{2\mathrm{D}\sigma} k^2 + i\pi}, \tag{3a}$$

$$f_{3\mathrm{D}\sigma}(k) \simeq \frac{1}{-a^{-1}_{3\mathrm{D}\sigma} + ik}, \tag{3b}$$

namely the 2D and 3D scattering lengths, $a_{2\mathrm{D}\sigma}$ and $a_{3\mathrm{D}\sigma}$, and a 2D range parameter $R_{2\mathrm{D}\sigma}$ [46,54]. The presence of $R_{2\mathrm{D}\sigma}$ in Eq. (3a) allows us to model the strongly energy-dependent scattering close to the ^{173}Yb orbital Feshbach resonance [45,55,56] in a 2D geometry. Conversely, we can safely neglect effective range corrections for the broad resonance, 3D case of ^{6}Li. In what follows, we take the impurity spin-$\uparrow$ (spin-$\downarrow$) state to be strongly (weakly) interacting with the medium [46], as depicted in Fig. 1. To simplify notation, we therefore identify $a_{3\mathrm{D}} \equiv a_{3\mathrm{D}\uparrow}$, $a_{2\mathrm{D}} \equiv a_{2\mathrm{D}\uparrow}$, and $R_{2\mathrm{D}} \equiv R_{2\mathrm{D}\uparrow}$.

The radio frequency [14] or optical [16] fields that couple the impurities in states $\uparrow$ and $\downarrow$ are described within the rotating wave approximation:

$$\hat{H}_\Omega = \frac{\Omega_0}{2} \sum_{\mathbf{k}} (\hat{c}^\dagger_{\mathbf{k}\downarrow} \hat{c}_{\mathbf{k}\uparrow} + \hat{c}^\dagger_{\mathbf{k}\uparrow} \hat{c}_{\mathbf{k}\downarrow}) + \Delta\omega\, \hat{n}_\downarrow. \tag{4}$$

Here, $\hat{n}_\sigma = \sum_{\mathbf{k}} (\hat{c}^\dagger_{\mathbf{k}\sigma} \hat{c}_{\mathbf{k}\sigma} + \hat{d}^\dagger_{\mathbf{k}\sigma} \hat{d}_{\mathbf{k}\sigma})$ is the spin-σ impurity number operator, Ω_0 is the (bare) Rabi coupling, and $\Delta\omega$ is the detuning from the bare $\downarrow - \uparrow$ transition.

Perturbative analysis.—We can gain insight into the nature of the repulsive Fermi polaron by analyzing the quasiparticle peak in the spectrum at weak interactions and temperature $T = 0$, such that the polaron is at rest. Focussing on the 3D case, in the limit $k_F a_{3\mathrm{D}} \ll 1$ the polaron energy E_+ is given by the mean-field expression

$E_+ = (4k_F a_{3D}/3\pi)E_F + O(a_{3D}^2)$ [57], where $E_F = (k_F^2/2m)$ is the Fermi energy with k_F the Fermi momentum. Thus, the quasiparticle state is pushed up into the continuum of scattering states that exists above zero energy in the case of attractive interactions. In particular, by performing a perturbative analysis [46], we find that the broadening of the quasiparticle peak [Fig. 1(b)] is dominated by the coupling to this continuum, such that the leading order behavior is

$$\Gamma \simeq \frac{8(k_F a_{3D})^4}{9\pi^3} E_F \simeq 0.029(k_F a_{3D})^4 E_F. \tag{5}$$

This has two important consequences. First, at orders below a_{3D}^4, the quasiparticle behavior is indistinguishable from the case of truly repulsive interactions, where the lifetime would be infinite [34,57]. In this regime, the repulsive polaron is adiabatically connected to the noninteracting impurity. Second, the contribution to the quasiparticle width from relaxation to the attractive branch is negligible in this limit, since it is dominated by three-body recombination [14] and takes the form $\Gamma_3 \simeq 0.025(k_F a_{3D})^6 E_F \ll \Gamma$ [58]. This illustrates that—within the perturbative regime—the finite quasiparticle lifetime arises from many-body dephasing processes that are manifestly distinct from relaxation to negative-energy states. Moreover, this cannot be viewed as momentum relaxation like in usual Fermi liquid theory [1], since we are considering a *zero-momentum* quasiparticle.

Rabi oscillations as a probe of quasiparticles.—We now argue that Rabi oscillations provide a sensitive probe of the repulsive polaron width (or quasiparticle lifetime). We focus on zero total momentum, since we are interested in decoherence effects beyond the standard momentum relaxation occurring in Fermi liquid theory [1]. At times $t \geq 0$, the impurity population in spin σ is

$$\mathcal{N}_\sigma(t) = \mathrm{Tr}[\hat{\rho}_0 \hat{c}(t) \hat{n}_\sigma \hat{c}^\dagger(t)], \tag{6}$$

where $\hat{c}(t)$ is the impurity operator in the Heisenberg picture. Here, our initial state $\hat{c}(t=0) = \hat{c}_{\mathbf{0}\downarrow}$ is chosen such that $\mathcal{N}_\downarrow(0) = 1$ and $\mathcal{N}_\uparrow(0) = 0$. The trace is over all states of the medium in the absence of the impurity, and we use the thermal density matrix $\hat{\rho}_0 = \exp(-\beta \hat{H}_0)/\mathrm{Tr}[\exp(-\beta \hat{H}_0)]$ with $\beta \equiv 1/T$ (we set the Boltzmann constant to 1). Under the assumption that $\hat{n}_\downarrow \simeq \hat{c}^\dagger_{\mathbf{0}\downarrow} \hat{c}_{\mathbf{0}\downarrow}$ (which would be true for impurities with infinite mass), we find [46]

$$\mathcal{N}_\downarrow(t) \simeq \int d\omega d\omega' \tilde{A}_\downarrow(\omega) \tilde{A}_\downarrow(\omega') e^{-i(\omega-\omega')t}, \tag{7}$$

where $\tilde{A}_\downarrow(\omega)$ is the spin-$\downarrow$ impurity spectral function in the presence of Rabi coupling. Taking the Rabi oscillations to be on resonance with the repulsive quasiparticle, i.e., $\Delta\omega = E_+$, we can furthermore approximate the spin-dependent impurity Green's functions in the absence of Rabi coupling as $G_\downarrow(\omega) \simeq 1/(\omega - E_+ + i\eta)$ and $G_\uparrow(\omega) \simeq Z/(\omega - E_+ + i\Gamma)$, where Z is the quasiparticle residue and η is a convergence factor that implicitly carries the limit $\eta \to 0^+$. With these approximations and as long as $\Gamma \lesssim \sqrt{Z}\Omega_0$, we finally obtain [46]

$$\mathcal{N}_\downarrow(t) \simeq e^{-\Gamma t}\left[\frac{1}{2} + \frac{1}{2}\cos\left(t\sqrt{\Omega_0^2 Z - \Gamma^2}\right)\right]. \tag{8}$$

Equation (8) provides two valuable insights. First, the Rabi oscillation frequency Ω is related to the residue via $Z \simeq (\Omega^2 + \Gamma^2)/\Omega_0^2$, which provides a correction to the standard approximation of $Z \simeq (\Omega/\Omega_0)^2$ [7]. Second, we see that the damping of Rabi oscillations is precisely the quasiparticle width Γ. This key result has been observed in experiment [14,16] but has previously lacked theoretical support.

Variational approach.—We now turn to modeling the experimental Rabi oscillations. We apply the finite-temperature variational approach developed in Ref. [44] in the context of Ramsey spectroscopy of impurities in a Fermi sea [13] (see also Ref. [59] for a related zero-temperature approach). The idea in this truncated basis method (TBM) is to introduce a time-dependent variational impurity operator $\hat{c}(t) = \hat{c}_\uparrow(t) + \hat{c}_\downarrow(t)$ that only approximately satisfies the Heisenberg equation of motion. This allows us to introduce an error operator $\hat{\epsilon}(t) \equiv i\partial_t \hat{c}(t) - [\hat{c}(t), \hat{H}]$ and an associated error quantity $\Delta(t) \equiv \mathrm{Tr}[\hat{\rho}_0 \hat{\epsilon}(t) \hat{\epsilon}^\dagger(t)]$. Our variational ansatz for the spin-σ component of the impurity operator is inspired by the work of Chevy [24] and corresponds to

$$\hat{c}_\sigma(t) = \alpha_0^\sigma(t)\hat{c}_{\mathbf{0}\sigma} + \sum_{\mathbf{k}} \alpha_{\mathbf{k}}^\sigma(t) \hat{f}^\dagger_{\mathbf{k}} \hat{d}_{\mathbf{k}\sigma} + \sum_{\mathbf{k},\mathbf{q}} \alpha_{\mathbf{kq}}^\sigma(t) \hat{f}^\dagger_{\mathbf{q}} \hat{f}_{\mathbf{k}} \hat{c}_{\mathbf{q}-\mathbf{k}\sigma}. \tag{9}$$

The variational operator consists of three terms: the bare impurity, the impurity bound to a fermion in a closed-channel dimer, and the impurity with a particle-hole excitation. The time dependence is entirely contained within the variational coefficients $\{\alpha\}$, allowing us to impose the minimization condition $\partial\Delta(t)/\partial\dot{\alpha}_j^{\sigma*}(t) = 0$. Since the Rabi coupling is suddenly turned on at $t = 0$, we can use the stationary solutions obtained from a set of linear equations for the expansion coefficients. This follows Ref. [44] with straightforward modifications due to the two possible impurity spin states [46].

Following the application of an external driving field, we obtain the Rabi oscillations within our variational approach via Eq. (6). We show the resulting Rabi oscillations in Fig. 2 for a representative set of interaction strengths and temperatures T/T_F in both two and three dimensions, where the Fermi temperature $T_F = E_F$. Here we set the

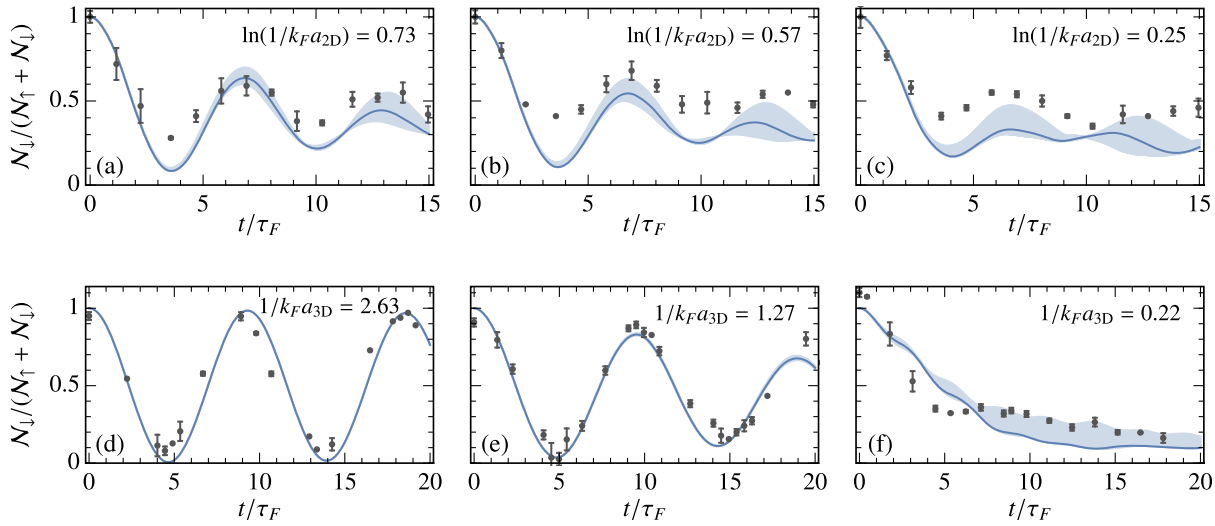

FIG. 2. Rabi oscillations calculated using the TBM (solid lines) and compared with the data (black dots) from the 2D ^{173}Yb experiment [16] (top row) and the 3D ^{6}Li experiment [14] (bottom row). In the top row, $\Omega_0/E_F \simeq 0.95$ and $T/T_F \simeq 0.16$ while, from left to right, $\ln(1/k_F a_{2D}) = 0.73, 0.57$, and 0.25. In the bottom row, $\Omega_0/E_F \simeq 0.68$ and $T/T_F \simeq 0.13$ while, from left to right, $1/(k_F a) = 2.63, 1.27$, and 0.22. The shaded regions correspond to the estimated uncertainty in the detuning around the repulsive polaron energy [46]. In the top row, the data is calculated from the sole measurement of $\mathcal{N}_\downarrow(t)$, and the normalization of each data point to $\mathcal{N}_\downarrow(t=0)$ [46]. We define the Fermi time $\tau_F \equiv 1/E_F$.

detuning to match the theoretical repulsive polaron energy, with a small shift due to initial state interactions [46]. The shaded regions illustrate the range of possible results that can be obtained by varying the detuning within the width of the repulsive polaron quasiparticle peak [46]. This accounts for the Rabi oscillations being slightly off resonance in the experiment due to the nonzero density of impurities, the density inhomogeneity within the trap, and other technical limitations.

Figure 2 demonstrates that our variational approach captures the Rabi oscillations between the bare impurity and the repulsive polaron in the 2D [16] and 3D [14] experiments. We note that there is a small positive offset in the 2D data [46], which does not strongly affect the extracted Rabi parameters. Crucially, our variational ansatz does not incorporate any processes where the repulsive polaron decays into the attractive branch, because these involve additional particle-hole excitations [35] which are neglected in Eq. (9). Therefore, the consistency between our theoretical results and the experiments provides strong evidence that the decoherence in the Rabi oscillations—and hence the inverse quasiparticle lifetime Γ—is physically dominated by the coupling to the continuum at positive energies, rather than by relaxation to the attractive branch. Given the fundamental differences between the two experiments [14,16], we expect this to be a generic feature of the mobile Fermi polaron with short-range attractive interactions.

Quasiparticle properties.—We can further quantify the nature of the repulsive polaron by determining the frequency Ω and damping Γ_R of the observed Rabi oscillations, which can be modeled approximately as [14]:

$$\mathcal{N}_\downarrow(t) \simeq b e^{-\Gamma_{\rm bg} t} + (1-b) e^{-\Gamma_R t}\cos(\Omega t). \tag{10}$$

Here, b is a dimensionless fitting parameter, while $\Gamma_{\rm bg}$ can be regarded as a background decay rate of the spin-$\downarrow$ state. We see that Eq. (10) reduces to our theoretical expression in Eq. (8) if we set $b = 1/2$ and $\Gamma_{\rm bg} = \Gamma_R$. In practice, we find that $\Gamma_{\rm bg} < \Gamma_R$ since there are scattering processes that can populate the spin-$\downarrow$ state without contributing to the damping of oscillations, and these are neglected in our approximation (7).

Using the fit provided in Eq. (10), we extract both Ω and Γ_R from our simulated Rabi oscillations within the TBM and compare them with the experimental results, as depicted in Fig. 3. We also show the repulsive polaron residue Z and inverse quasiparticle lifetime Γ obtained directly from the impurity Green's function $G_\downarrow(\omega)$, where the impurity self energy is calculated using ladder diagrams [46]. Such an approach is equivalent to our spin-$\downarrow$ variational ansatz in Eq. (9) in the absence of Rabi coupling [44], and similarly it does not include the contribution to the quasiparticle lifetime due to relaxation from the repulsive branch to lower lying states.

Referring to Fig. 3, we see that all three methods are in good agreement with each other for weak to intermediate interaction strengths. This is particularly evident for Γ_R in Fig. 3(d), where the agreement spans two orders of magnitude. Here we find that the finite temperature of the Fermi gas leads to deviations from the perturbative result in Eq. (5), but the behavior is still markedly different from the momentum relaxation predicted by Fermi liquid theory [11]. The observed agreement suggests that

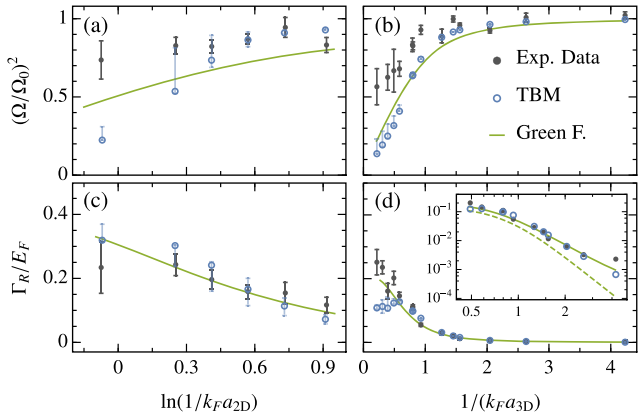

FIG. 3. The extracted frequency $(\Omega/\Omega_0)^2$ and damping Γ_R of the Rabi oscillations as determined from the TBM (blue circles) and in the 2D (a),(c) and 3D (b),(d) experiments (black dots). The TBM error bars are derived from the uncertainty in detuning [46], which tends to increase the oscillation frequency. The extracted Rabi parameters are also compared with the quasiparticle residue $Z \simeq (\Omega/\Omega_0)^2$ (top row) and quasiparticle inverse lifetime $\Gamma \simeq \Gamma_R$ (bottom row) obtained directly from the finite-temperature impurity Green's function (green solid line). The TBM simulations are set to match the experimental parameters [46]. Inset: data in (d) plotted on a log-log scale, together with the result of a zero-temperature Green's function calculation (green dashed line).

temperature predominantly affects the many-body dephasing via thermal fluctuations of the medium rather than through finite impurity momenta. In Fig. 3(a), the slightly elevated values of $(\Omega/\Omega_0)^2$ compared to the expected residue Z can be attributed to the strong Rabi driving ($\Omega_0/E_F \gtrsim 1$), such that the oscillation period approaches the formation time of the polaron.

At stronger repulsive interactions, there are more pronounced deviations as the repulsive polaron quasiparticle becomes less well defined and the effects of a finite impurity density in experiments are expected to be more important [14]. In particular, it becomes increasingly difficult to extract quasiparticle properties from the Rabi oscillations once the quasiparticle width Γ is comparable to Ω, which is consistent with our theoretical analysis in Eq. (8). This accounts for the suppression of coherent oscillations in Fig. 2(f) as well as the anomalously low Γ_R obtained from the TBM near unitarity in Fig. 3(d). Our results suggest that one could better probe the repulsive polaron quasiparticle lifetime at strong coupling by increasing the Rabi drive Ω_0.

Conclusions.—We have investigated the nature of the repulsive Fermi polaron in two and three dimensions. We have shown that both the quasiparticle lifetime and the residue can be probed by driving Rabi oscillations between weakly and strongly interacting impurity spin states. By simulating the Rabi oscillations in two fundamentally different experiments and by performing a perturbative analysis of the weak-coupling limit, we have demonstrated that the quasiparticle lifetime is determined by many-body dephasing within the upper repulsive branch and is thus typically much shorter than the lifetime of the repulsive branch itself. Our work provides an important benchmark for many-body numerical approaches [60] and it opens up the prospect of exploring a long-lived repulsive Fermi gas with novel excitations beyond the Fermi liquid paradigm.

We are grateful to J. Cole, P. Massignan, A. Recati, and M. Zonnios for useful discussions. J. L., W. E. L., and M. M. P. acknowledge support from the Australian Research Council Centre of Excellence in Future Low-Energy Electronics Technologies (Grant No. CE170100039). J. L. is also supported through the Australian Research Council Future Fellowship FT160100244. N. D. O. acknowledges funding from the Max-Planck-Gesellschaft. M. Z. was supported by the ERC through Grant No. 637738 PoLiChroM. F. S. acknowledges funding from EU H2020 programme under the Marie Skłodowska-Curie GA Grant No. 705269 and Fondazione Cassa di Risparmio di Firenze Project No. QuSim2D 2016.0770.

[1] P. Nozières and D. Pines, *Theory of Quantum Liquids*, Advanced Books Classics (W. A. Benjamin, New York, 1966).
[2] C. Varma, Z. Nussinov, and W. van Saarloos, Singular or non-Fermi liquids, Phys. Rep. **361**, 267 (2002).
[3] M. R. Norman, The challenge of unconventional superconductivity, Science **332**, 196 (2011).
[4] P. Massignan, M. Zaccanti, and G. M. Bruun, Polarons, dressed molecules and itinerant ferromagnetism in ultracold Fermi gases, Rep. Prog. Phys. **77**, 034401 (2014).
[5] A. Schirotzek, C.-H. Wu, A. Sommer, and M. W. Zwierlein, Observation of Fermi Polarons in a Tunable Fermi Liquid of Ultracold Atoms, Phys. Rev. Lett. **102**, 230402 (2009).
[6] S. Nascimbène, N. Navon, K. J. Jiang, L. Tarruell, M. Teichmann, J. McKeever, F. Chevy, and C. Salomon, Collective Oscillations of an Imbalanced Fermi Gas: Axial Compression Modes and Polaron Effective Mass, Phys. Rev. Lett. **103**, 170402 (2009).
[7] C. Kohstall, M. Zaccanti, M. Jag, A. Trenkwalder, P. Massignan, G. Bruun, F. Schreck, and R. Grimm, Metastability and coherence of repulsive polarons in a strongly interacting Fermi mixture, Nature (London) **485**, 615 (2012).
[8] M. Koschorreck, D. Pertot, E. Vogt, B. Fröhlich, M. Feld, and M. Köhl, Attractive and repulsive Fermi polarons in two dimensions, Nature (London) **485**, 619 (2012).
[9] Y. Zhang, W. Ong, I. Arakelyan, and J. E. Thomas, Polaron-to-Polaron Transitions in the Radio-Frequency Spectrum of a Quasi-Two-Dimensional Fermi Gas, Phys. Rev. Lett. **108**, 235302 (2012).
[10] A. N. Wenz, G. Zürn, S. Murmann, I. Brouzos, T. Lompe, and S. Jochim, From few to many: Observing the formation of a Fermi sea one atom at a time, Science **342**, 457 (2013).
[11] M. Cetina, M. Jag, R. S. Lous, J. T. M. Walraven, R. Grimm, R. S. Christensen, and G. M. Bruun, Decoherence of

Impurities in a Fermi Sea of Ultracold Atoms, Phys. Rev. Lett. **115**, 135302 (2015).
[12] W. Ong, C. Cheng, I. Arakelyan, and J. E. Thomas, Spin-Imbalanced Quasi-Two-Dimensional Fermi Gases, Phys. Rev. Lett. **114**, 110403 (2015).
[13] M. Cetina, M. Jag, R. S. Lous, I. Fritsche, J. T. M. Walraven, R. Grimm, J. Levinsen, M. M. Parish, R. Schmidt, M. Knap, and E. Demler, Ultrafast many-body interferometry of impurities coupled to a Fermi sea, Science **354**, 96 (2016).
[14] F. Scazza, G. Valtolina, P. Massignan, A. Recati, A. Amico, A. Burchianti, C. Fort, M. Inguscio, M. Zaccanti, and G. Roati, Repulsive Fermi Polarons in a Resonant Mixture of Ultracold 6-Li Atoms, Phys. Rev. Lett. **118**, 083602 (2017).
[15] Z. Yan, P. B. Patel, B. Mukherjee, R. J. Fletcher, J. Struck, and M. W. Zwierlein, Boiling a Unitary Fermi Liquid, Phys. Rev. Lett. **122**, 093401 (2019).
[16] N. Darkwah Oppong, L. Riegger, O. Bettermann, M. Höfer, J. Levinsen, M. M. Parish, I. Bloch, and S. Fölling, Observation of Coherent Multiorbital Polarons in a Two-Dimensional Fermi Gas, Phys. Rev. Lett. **122**, 193604 (2019).
[17] G. Ness, C. Shkedrov, Y. Florshaim, O. K. Diessel, J. von Milczewski, R. Schmidt, and Y. Sagi, Observation of a smooth polaron-molecule transition in a degenerate Fermi gas, arXiv:2001.10450.
[18] J. Catani, G. Lamporesi, D. Naik, M. Gring, M. Inguscio, F. Minardi, A. Kantian, and T. Giamarchi, Quantum dynamics of impurities in a one-dimensional Bose gas, Phys. Rev. A **85**, 023623 (2012).
[19] M.-G. Hu, M. J. Van de Graaff, D. Kedar, J. P. Corson, E. A. Cornell, and D. S. Jin, Bose Polarons in the Strongly Interacting Regime, Phys. Rev. Lett. **117**, 055301 (2016).
[20] N. B. Jørgensen, L. Wacker, K. T. Skalmstang, M. M. Parish, J. Levinsen, R. S. Christensen, G. M. Bruun, and J. J. Arlt, Observation of Attractive and Repulsive Polarons in a Bose-Einstein Condensate, Phys. Rev. Lett. **117**, 055302 (2016).
[21] F. Camargo, R. Schmidt, J. D. Whalen, R. Ding, G. Woehl, S. Yoshida, J. Burgdörfer, F. B. Dunning, H. R. Sadeghpour, E. Demler, and T. C. Killian, Creation of Rydberg Polarons in a Bose Gas, Phys. Rev. Lett. **120**, 083401 (2018).
[22] Z. Z. Yan, Y. Ni, C. Robens, and M. W. Zwierlein, Bose polarons near quantum criticality, Science **368**, 190 (2020).
[23] M. Sidler, P. Back, O. Cotlet, A. Srivastava, T. Fink, M. Kroner, E. Demler, and A. Imamoglu, Fermi polaron-polaritons in charge-tunable atomically thin semiconductors, Nat. Phys. **13**, 255 (2017).
[24] F. Chevy, Universal phase diagram of a strongly interacting Fermi gas with unbalanced spin populations, Phys. Rev. A **74**, 063628 (2006).
[25] R. Combescot, A. Recati, C. Lobo, and F. Chevy, Normal State of Highly Polarized Fermi Gases: Simple Many-Body Approaches, Phys. Rev. Lett. **98**, 180402 (2007).
[26] N. Prokof'ev and B. Svistunov, Fermi-polaron problem: Diagrammatic Monte Carlo method for divergent sign-alternating series, Phys. Rev. B **77**, 020408(R) (2008).
[27] R. Combescot and S. Giraud, Normal State of Highly Polarized Fermi Gases: Full Many-Body Treatment, Phys. Rev. Lett. **101**, 050404 (2008).
[28] M. Punk, P. T. Dumitrescu, and W. Zwerger, Polaron-to-molecule transition in a strongly imbalanced Fermi gas, Phys. Rev. A **80**, 053605 (2009).
[29] C. J. M. Mathy, M. M. Parish, and D. A. Huse, Trimers, Molecules, and Polarons in Mass-Imbalanced Atomic Fermi Gases, Phys. Rev. Lett. **106**, 166404 (2011).
[30] R. Schmidt and T. Enss, Excitation spectra and rf response near the polaron-to-molecule transition from the functional renormalization group, Phys. Rev. A **83**, 063620 (2011).
[31] C. Trefzger and Y. Castin, Impurity in a Fermi sea on a narrow Feshbach resonance: A variational study of the polaronic and dimeronic branches, Phys. Rev. A **85**, 053612 (2012).
[32] J. Levinsen and M. M. Parish, Strongly interacting two-dimensional Fermi gases, Annu. Rev. Cold At. Mol. **3**, 1 (2015).
[33] X. Cui and H. Zhai, Stability of a fully magnetized ferromagnetic state in repulsively interacting ultracold Fermi gases, Phys. Rev. A **81**, 041602(R) (2010).
[34] S. Pilati, G. Bertaina, S. Giorgini, and M. Troyer, Itinerant Ferromagnetism of a Repulsive Atomic Fermi Gas: A Quantum Monte Carlo Study, Phys. Rev. Lett. **105**, 030405 (2010).
[35] P. Massignan and G. M. Bruun, Repulsive polarons and itinerant ferromagnetism in strongly polarized Fermi gases, Eur. Phys. J. D **65**, 83 (2011).
[36] O. Goulko, A. S. Mishchenko, N. Prokof'ev, and B. Svistunov, Dark continuum in the spectral function of the resonant Fermi polaron, Phys. Rev. A **94**, 051605(R) (2016).
[37] H. Tajima and S. Uchino, Many Fermi polarons at nonzero temperature, New J. Phys. **20**, 073048 (2018).
[38] B. C. Mulkerin, X.-J. Liu, and H. Hu, Breakdown of the Fermi polaron description near Fermi degeneracy at unitarity, Ann. Phys. (Berlin) **407**, 29 (2019).
[39] D. Pekker, M. Babadi, R. Sensarma, N. Zinner, L. Pollet, M. W. Zwierlein, and E. Demler, Competition between Pairing and Ferromagnetic Instabilities in Ultracold Fermi Gases near Feshbach Resonances, Phys. Rev. Lett. **106**, 050402 (2011).
[40] C. Sanner, E. J. Su, W. Huang, A. Keshet, J. Gillen, and W. Ketterle, Correlations and Pair Formation in a Repulsively Interacting Fermi Gas, Phys. Rev. Lett. **108**, 240404 (2012).
[41] G. Valtolina, F. Scazza, A. Amico, A. Burchianti, A. Recati, T. Enss, M. Inguscio, M. Zaccanti, and G. Roati, Exploring the ferromagnetic behaviour of a repulsive Fermi gas through spin dynamics, Nat. Phys. **13**, 704 (2017).
[42] A. Amico, F. Scazza, G. Valtolina, P. E. S. Tavares, W. Ketterle, M. Inguscio, G. Roati, and M. Zaccanti, Time-Resolved Observation of Competing Attractive and Repulsive Short-Range Correlations in Strongly Interacting Fermi Gases, Phys. Rev. Lett. **121**, 253602 (2018).
[43] F. Scazza, G. Valtolina, A. Amico, P. E. S. Tavares, M. Inguscio, W. Ketterle, G. Roati, and M. Zaccanti, Exploring emergent heterogeneous phases in strongly repulsive Fermi gases, Phys. Rev. A **101**, 013603 (2020).
[44] W. E. Liu, J. Levinsen, and M. M. Parish, Variational Approach for Impurity Dynamics at Finite Temperature, Phys. Rev. Lett. **122**, 205301 (2019).

[45] R. Zhang, Y. Cheng, H. Zhai, and P. Zhang, Orbital Feshbach Resonance in Alkali-Earth Atoms, Phys. Rev. Lett. **115**, 135301 (2015).

[46] See the Supplemental Material at http://link.aps.org/supplemental/10.1103/PhysRevLett.125.133401 for details of the model and scattering parameters, the variational approach, the perturbative analysis, and the relationship between Rabi oscillations and the quasiparticle width. This includes a table of experimental parameters used for the TBM simulations, as well as Refs. [47–51].

[47] J. Xu, R. Zhang, Y. Cheng, P. Zhang, R. Qi, and H. Zhai, Reaching a Fermi-superfluid state near an orbital Feshbach resonance, Phys. Rev. A **94**, 033609 (2016).

[48] T. Kirk and M. M. Parish, Three-body correlations in a two-dimensional SU(3) Fermi gas, Phys. Rev. A **96**, 053614 (2017).

[49] V. Gurarie and L. Radzihovsky, Resonantly paired fermionic superfluids, Ann. Phys. (Berlin) **322**, 2 (2007).

[50] D. S. Petrov and G. V. Shlyapnikov, Interatomic collisions in a tightly confined Bose gas, Phys. Rev. A **64**, 012706 (2001).

[51] I. Bloch, J. Dalibard, and W. Zwerger, Many-body physics with ultracold gases, Rev. Mod. Phys. **80**, 885 (2008).

[52] W. E. Liu, Z.-Y. Shi, J. Levinsen, and M. M. Parish, Radio-Frequency Response and Contact of Impurities in a Quantum Gas, Phys. Rev. Lett. **125**, 065301 (2020).

[53] W. E. Liu, Z.-Y. Shi, M. M. Parish, and J. Levinsen, Theory of radio-frequency spectroscopy of impurities in quantum gases, Phys. Rev. A **102**, 023304 (2020).

[54] J. Levinsen and M. M. Parish, Bound States in a Quasi-Two-Dimensional Fermi Gas, Phys. Rev. Lett. **110**, 055304 (2013).

[55] M. Höfer, L. Riegger, F. Scazza, C. Hofrichter, D. R. Fernandes, M. M. Parish, J. Levinsen, I. Bloch, and S. Fölling, Observation of an Orbital Interaction-Induced Feshbach Resonance in ^{173}Yb, Phys. Rev. Lett. **115**, 265302 (2015).

[56] G. Pagano, M. Mancini, G. Cappellini, L. Livi, C. Sias, J. Catani, M. Inguscio, and L. Fallani, Strongly Interacting Gas of Two-Electron Fermions at an Orbital Feshbach Resonance, Phys. Rev. Lett. **115**, 265301 (2015).

[57] R. Bishop, On the ground state of an impurity in a dilute fermi gas, Ann. Phys. (Berlin) **78**, 391 (1973).

[58] D. S. Petrov, Three-body problem in Fermi gases with short-range interparticle interaction, Phys. Rev. A **67**, 010703(R) (2003).

[59] M. M. Parish and J. Levinsen, Quantum dynamics of impurities coupled to a Fermi sea, Phys. Rev. B **94**, 184303 (2016).

[60] O. Goulko, A. S. Mishchenko, L. Pollet, N. Prokof'ev, and B. Svistunov, Numerical analytic continuation: Answers to well-posed questions, Phys. Rev. B **95**, 014102 (2017).